



Published in final edited form as:

Anal Chem. 1998 September 1; 70(17): 3517–3524.

Separation and Characterization of Amines from Individual Atrial Gland Vesicles of *Aplysia californica*

Sheri J. Lillard^{†,‡}, Daniel T. Chiu[†], Richard H. Scheller[§], and Richard N. Zare^{*†}

Departments of Chemistry and Molecular and Cellular Physiology, Howard Hughes Medical Institute, Stanford University, Stanford, California 94305

Sandra E. Rodríguez-Cruz and Evan R. Williams

Department of Chemistry, University of California, Berkeley, California 94720

Owe Orwar^{||}, Mats Sandberg[⊥], and J. Anders Lundqvist^{||}

Department of Chemistry, Göteborg University, SE-412 96, and Department of Anatomy and Cell Biology, Göteborg University, SE-413 90, Göteborg, Sweden

Abstract

Several amine-containing components of individual vesicles from the atrial gland of *Aplysia californica* were identified with capillary electrophoresis (CE). On-line derivatization with naphthalene-2,3-dicarboxaldehyde was performed, and the derivatized amine-containing components were detected with laser-induced fluorescence (LIF). Amino acids, including taurine, that had not been determined previously in atrial gland vesicles were observed by using CE-LIF, and their identities were confirmed with CE, HPLC, NMR, and electrospray ionization mass spectrometry. The finding that taurine is packaged and stored into secretory vesicles supports the hypothesis that taurine may exhibit neuromodulatory activity. The bioactive peptides, well-known to be in atrial gland vesicles, were detected in lysed vesicle samples fractionated with HPLC and analyzed by matrix-assisted laser desorption/ionization time-of-flight mass spectrometry. These peptides were also observed in single-vesicle runs with CE-LIF. The atrial gland vesicles (ranging from 0.5 to 2 μm diameter and 65 aL to 4 fL volume, respectively) studied in this work represent the smallest biological entities to be analyzed chemically on an individual basis.

The goal of analyzing individual biological cells has been realized with various microanalytical techniques. The motivation behind studying this specialized sample type is the heterogeneity that is present in the cell populations that comprise tissues. The measurement of an average value for a specific parameter of a population does not necessarily reflect the range of values resulting from individual members of the population. Although ensemble measurements can reveal abnormalities in a cell population, these measurements do not indicate intercellular differences that may provide more important clues about the history or future of a cell.

Reports of single-cell analyses date back to the 1950s, in which single neurons were studied.^{1–4} Since that time, several methods, including separations, have been used to analyze single cells.^{5–23} Owing to its high sensitivity, laser-induced fluorescence (LIF) has played a significant role in the chemical analysis of individual cells with capillary electrophoresis (CE),^{5,6} including wavelength-resolved LIF of neurotransmitters in single neurons.⁷ Novel analyses of single cells with CE include cytoplasmic sampling from⁸ and transporting solutes into⁹

[†]Department of Chemistry, Stanford University.

Present address: Department of Chemistry, University of California, Riverside, CA 92521.

[§]Department of Molecular and Cellular Physiology, Stanford University.

^{||}Department of Chemistry, Göteborg University.

[⊥]Department of Anatomy and Cell Biology, Göteborg University.

Xenopus oocytes, monitoring release,^{10–12} and measuring apoptosis.¹³ In addition to LIF, other successful detection schemes for single-cell CE include electro-chemistry,¹⁴ mass spectrometry,¹⁵ and absorbance.¹⁶ Matrix-assisted laser desorption/ionization time-of-flight (MALDI-TOF) mass spectrometry has been used recently to investigate proteolytic processing of peptides in single neurons from *Aplysia*.¹⁷

Interest in analyzing individual biological entities has extended from the realm of the single cell to that of subcellular components. Microelectrodes, when placed in proximity to the surface of a cell, have been used to detect released components, including those corresponding to single vesicles.^{18–20} Another electrochemical-based method, patch amperometry, has been used to monitor exocytosis and secretion at the level of a single vesicle.²¹ In addition, static imaging of cultured mast cells (RBL-2H3) based on three-photon excitation²² and real-time exocytosis of isolated mast cells using native fluorescence (single-photon excitation)²³ have revealed fluorescence most likely from single granules.

The electrochemical and imaging techniques described above detect components believed to be from single vesicles. However, those measurements were made on isolated cells rather than on precisely manipulated individual vesicles. Recently, we have demonstrated the injection, separation, and detection of components from single secretory vesicles.²⁴ In the present work, we describe the identification, characterization, and biological significance of the amine-containing molecules in single atrial gland vesicles from the sea mollusk *Aplysia californica*.

EXPERIMENTAL SECTION

Reagents.

All chemicals were from Mallinckrodt (Paris, KY) unless otherwise specified. KCN and KCl were from J. T. Baker, Inc. (Phillipsburg, NJ), and acetonitrile was obtained from Fisher (Fairlawn, NJ). Amino acids were from Sigma Chemical (St. Louis, MO). All solutions for CE-LIF, including buffers, naphthalene-2,3-dicarboxaldehyde (NDA) dilutions, vesicle extracts, and off-column derivatization reactions, were prepared and stored in glass vials. These glass vials were also used to contain the running buffer for CE-LIF. Sodium tetraborate solutions were prepared with an unadjusted pH ~9.

NDA that was used in all experiments was obtained from Molecular Probes (Eugene, OR). Stock concentrations of NDA (100 mM in acetonitrile) and KCN (100 mM in 10 mM sodium tetraborate) were prepared every 2–3 days and kept at room temperature in the dark. Dilutions of stock solutions of NDA (10 mM in acetonitrile) and KCN (1.1 mM in 10 mM borate) were prepared every day. NDA/CN⁻ reaction mixtures were prepared before each run by mixing 10 μ L of 10 mM NDA with 90 μ L of 1.1 mM KCN to give final concentrations of 1 mM each of NDA and KCN.

Dissection and Vesicle Isolation.

A. californica (200–600 g) were obtained from the University of Miami Aplysia facility (Miami, FL). The location of the atrial gland and the formation of the atrial gland peptides from their precursors in *Aplysia* are shown in Figure 1. Animals were anesthetized by injecting 2–3 times body weight of 390 mM MgCl₂ into the animal and waiting ~10 min before dissection. The animal was secured with dissecting pins, an incision was made in the foot at the abdominal region, and the atrial gland, which is a few millimeters in diameter, was removed from the distal end of the hermaphroditic duct. The gland was placed in 50–100 μ L of isotonic NaCl (711 mM NaCl and 10 mM NaH₂PO₄, pH 7.4), and the vesicles were dislodged by pressing on the gland with a razor blade or tweezers. This solution containing the vesicles was aspirated and placed in a microcentrifuge vial, and the procedure was repeated 1 or 2 times. The resulting vesicle suspension contained intact vesicles. To obtain lysed vesicles for

characterization studies on populations, the above procedure was performed except that a 50% methanol solution in deionized water (Sigma, endotoxin-free) was used, instead of isotonic NaCl, to lyse the vesicles.

Injection of Single Vesicles and On-Column Derivatization.

A single-beam optical trap was used to control and manipulate individual vesicles and facilitate their introduction into the inlet of the tapered separation capillary. The optical trap was built in-house (Figure 2A) and has been described previously.²⁵ The output of a single-mode MOPA laser diode (model SDL-5762-A6, SDL, Inc., San Jose, CA) was sent through a spatial filter (model 900, Newport Corp., Irvine, CA) and then reflected from a near-IR mirror. The beam was then passed through a dichroic mirror and reflected from a polychroic mirror (Chroma Technology Corp., Brattleboro, VT) that was placed in the filter cube mount of an inverted microscope (Nikon Diaphot, Technical Instrument Co., San Francisco, CA). Subsequently, the beam was brought to a diffraction-limited focus with a high numerical aperture objective (100 \times , NA 1.4; Nikon model 85025, Technical Instrument Co.). The images of the capillary inlet and the vesicles were sent to a high-sensitivity SIT camera (Hamamatsu, model C2400-08, Technical Instrument Co.) that was mounted to the front port of the microscope. The images detected by the camera were displayed on a video screen and recorded by a VCR (model SVO-1500, Technical Instrument Co.).

For vesicle injection, a plug of isotonic NaCl was first injected (27 kV, 5 s) into the capillary to prevent vesicle lysis before the derivatizing solution was introduced. The outlet end of the capillary was raised a few millimeters relative to the vesicle droplet to create a slight outward pressure. A very dilute suspension of vesicles was placed on a cover slip, and the microscope stage was moved to search for and direct a vesicle to the optical trap (Figure 2B). The capillary was then positioned so that the vesicle was at the inlet (Figure 2C). Low voltage (0.5 kV) was applied, and the trap was turned off so that the vesicle entered the capillary (Figure 2D). Fine adjustment of voltage and pressure was performed for optimal injection.

On-column derivatization was performed as shown in Figure 3. Following injection of the vesicle (Figure 3A), the tapered inlet of the capillary was placed in the NDA solution (1 mM each NDA and KCN in 10 mM borate) which was electrokinetically injected (3.3 kV, 60 s) (Figure 3B). The vesicle was allowed to lyse and its contents were allowed to react for 5 min (Figure 3C), the inlet was returned to its buffer vial, and electrophoresis was initiated to separate the labeled components (Figure 3D). Off-column derivatization for CE-LIF utilized 10 μ L of vesicle extract mixed with 90 μ L of NDA solution that was allowed to react for 5 min prior to injection.

Separation and Detection (CE-LIF).

The setup for CE was home-built and has been described elsewhere.²⁵ Bare fused-silica capillaries were used (Polymicro Technologies, Phoenix, AZ) with dimensions of ~100-cm total length, 25- μ m i.d., and 150- μ m o.d. For single-vesicle runs, the inlet was tapered to facilitate injection and on-column derivatization.²⁵ Tapering was achieved by first fixing the end of the capillary to a laboratory bench with tape and then heating a section a few centimeters away from the fixed end with a butane flame. As the polyimide coating started to burn and the fused-silica started to soften, the capillary was pulled by hand. This procedure yielded highly polished capillary inlets with variable tip diameters.

High voltage (Glassman High Voltage, Inc., Whitehouse Station, NJ) for separation was 27 kV, for vesicle injection was 0.5 kV, and for NDA introduction was 3.3 kV. The running buffer consisted of 25% acetonitrile (Fisher, Fair Lawn, NJ) and 75% 50 mM sodium tetraborate, pH ~9 and was filtered with a 0.2- μ m syringe filter (Nalge Co., Rochester, NY) before use. At the

beginning of each day, capillaries were flushed with running buffer and were equilibrated at 27 kV for ~5 min. No other routine capillary treatment was performed. The 457-nm output of an argon ion laser (Spectra Physics, Mountain View, CA) was used to excite NDA fluorescence in the single-vesicle runs. Characterization studies of lysed vesicle extracts with CE-LIF, used a similar home-built system in which the 442-nm line of a He–Cd laser (Series 56, model 2056-3/15, Omnicrome, Chino, CA) was used as the excitation source for LIF. Electropherograms were collected using LabCalc (Galactic Industries, Salem, NH).

Electrospray Mass Spectrometry.

Samples of the vesicle contents were fractionated using size exclusion chromatography. Vesicle lysate (in methanolic water) was run through a Bio-Rad Econo-Pac 10DG (Bio-Gel P-6DG) column, which has an exclusion limit of 6000 Da and a fractionation range of 1000–6000 Da. Deionized water was used as the eluent, and aqueous fractions of both NDA-derivatized and underivatized samples were collected and mass analyzed using electrospray ionization with quadrupole mass spectrometry. The aqueous fractions were electrosprayed from an aluminum-clad, fused-silica capillary (Scientific Instrument Services, Inc., Ringoes, NJ) with a 100- μm i.d. The solution flow rate was 1.5 $\mu\text{L}/\text{min}$. The quadrupole instrument is a Hewlett-Packard 5989x spectrometer that has been modified by adding an electrospray ion source with two stages of differential pumping and an octopole ion guide. Ions are introduced through a heated metal capillary which is 12 cm long and has an inner diameter of 0.50 mm. The ion beam is skimmed with two 90° skimmers. The first and second skimmers have diameters of 1.0 and 2.0 mm, respectively. The pressure in the first and second stages is 1.3 Torr and 60 mTorr, respectively. The potentials applied to the capillary, skimmer 1, and skimmer 2 are approximately 23, 10, and 5 V, respectively. The potential of a cylindrical lens between the heated metal capillary and the first skimmer is typically ~70 V. A 29-cm-long octopole ion guide is used to transfer the ions from the source to the quadrupoles for mass analysis. This octopole operates at 2.0 MHz (50 $V_{\text{p-p}}$, 0 V dc offset). A set of lenses focuses the ions from the exit of the octopole ion guide into the quadrupoles. Five scans were averaged for each fraction. A total of ~8 μL of sample was consumed for each spectrum.

Details of the external ion source electrospray ionization Fourier transform mass spectrometer are described elsewhere.^{26,27} Spectra were acquired using a data acquisition rate of 5.3 MHz (cutoff corresponding to a lower m/z limit of 16) and a total of 128K data points were collected. Accurate mass measurements were made using internal standards. Arginine, heptylamine, and rubidium (m/z 84.9118, 72.17% abundance; m/z 86.9092, 27.83% abundance) were added to the vesicle sample. From a four-point calibration, the molecular weights of the LMCs (positive-ion mode) were determined with an average error of less than 10 ppm (95% confidence limit). The elemental compositions of these ions were determined from the masses of the common elements using a mass tolerance of 20 ppm and constrained by the measured isotope distributions.

MALDI-TOF Mass Spectrometry.

Lysed vesicle samples were fractionated with gradient elution HPLC using a procedure slightly modified from the literature.²⁸ Collected fractions were analyzed using (MALDI-TOF) mass spectrometry. Experiments were performed on a Voyager-DE RP Biospectrometry instrument (Perceptive Biosystems, Framingham, MA) in linear mode. A nitrogen laser (337 nm) was used for desorption, and scans were acquired in positive-ion mode. Matrixes were either α -cyano-4-hydroxycinnamic acid or sinapinic acid.

RESULTS AND DISCUSSION

NDA Derivatization.

NDA is a fluorogenic reagent that reacts with primary amines in the presence of a nucleophile (e.g., cyanide or 2-mercaptoethanol) and basic pH to form a fluorescent product.^{29,30} Our on-column derivatization scheme for amines released from lysed single vesicles is similar to that described by Gilman and Ewing.³¹ However, in our experiment, the derivatization volume inside the capillary inlet was significantly reduced because of tapering.

In Figure 4, the peak at ~12 min is present in blank (i.e., NDA/CN⁻ only) and vesicle runs. Although we made several attempts to reduce contamination and eliminate this peak, we were unsuccessful. Therefore, it was used as an electrophoretic marker to normalize migration times of the peaks from lysed and single vesicles. Interestingly, the same peak was observed by Gilman and Ewing,³¹ in which borate reaction and running buffers were also used. These authors attributed the peak to a neutral impurity.²⁴ Because the peak is present in completely independent experiments, it is unlikely that the peak is from a laboratory contaminant. A nonanalyte peak was also observed by Lunte and co-workers³² in a study of NDA-derivatized glutamate and aspartate, in which a borate reaction buffer was also used. In this case, the peak was present when either borate or Tris running buffers were used, with Tris buffer resulting in a much higher intensity for this peak. We believe that our peak at 12 min is caused by formation of fluorescent benzoin condensation products³³ or other side products³⁴ of NDA upon exposure to aqueous buffer conditions.

In our study, the vesicles were originally isolated and stored in a solution of artificial seawater (ASW),³⁵ at pH 7.6 composed of 490 mM NaCl, 11 mM KCl, 19 mM MgCl₂, 30 mM MgSO₄, 11 mM CaCl₂, and 10 mM Tris-HCl. However, we observed that NDA/CN⁻ in ASW (without vesicles present) turned yellowish-green, which indicates an NDA reaction. In fact, we observed background disturbances and extraneous peaks when this blank mixture was run by CE. The reaction was attributed to the Tris component in ASW, since NDA/CN⁻ in Tris only (without the other components) exhibited the same behavior. Thus, vesicles were isolated in isotonic NaCl for all single-vesicle experiments.

Analysis of Vesicle Components.

Figure 4A is an electropherogram of a lysed vesicle population obtained with CE-LIF. The major components are identified as NDA, N-terminal peptides (NTPs), leucine/isoleucine, alanine, taurine, and an unidentified component (peak 4). The details of characterization and identification are discussed in the following subsections. Parts B and C of Figure 4 are electropherograms resulting from the injection of individual vesicles.

Low-Mass Amines.—Previously, we found by HPLC analysis of a lysed vesicle extract, compared to a mixture of amino acid standards, that taurine was the major low-mass component of an atrial gland sample of a population of vesicles.²⁴ The presence of taurine was confirmed by spiking the vesicle sample with a taurine standard, and recoveries of 104–105% were obtained. Further confirmation of taurine was achieved by recording ¹H NMR spectra of a vesicle lysate sample fractionated with size exclusion chromatography and comparing this to a taurine standard. Vesicle samples were spiked with alanine, leucine, and isoleucine, reacted with NDA/CN⁻ and analyzed by CE with UV absorbance at 254 nm (data not shown). The most abundant low-mass amine was confirmed as taurine, and alanine and leucine/isoleucine was identified as shown in Figure 4.

Electrospray Mass Spectrometry.—All mass measurements were performed on vesicle lysate that was first run through a size exclusion column, as described in Experimental

Methods. The 6000-Da cutoff did not provide high selectivity, but the fractionation range (1000–6000 Da) did allow the lower mass compounds to be separated from the higher mass peptides and other compounds.

Previously we found that, in positive-ion mode, the most abundant masses of underivatized lysate were 117, 131, 132, and 143.²⁴ We also obtained molecular formulas from accurate mass measurements using an external ESI interface to a Fourier transform mass spectrometer.²⁴ While the mass and formula of 117 correspond to valine, the fragmentation pattern of a valine standard did not match the mass 117 component of our sample, indicating that it is an isomer of valine. Mass 131 was assigned to leucine/isoleucine, based on chemical formula and the presence of leucine/isoleucine in vesicle lysate analyzed with HPLC²⁴ and CE. Masses 132 and 143 remain unidentified.

Mass spectra of fractionated vesicle lysate were acquired in negative-ion mode for additional confirmation of the presence of taurine. Taurine ($\text{H}_2\text{NCH}_2\text{CH}_2\text{SO}_3\text{H}$) has a significantly lower response in positive-ion mode. A representative scan of fractionated vesicle lysate is shown in Figure 5A and is compared to a taurine standard, which is shown in Figure 5B. The peak at m/z 124 is consistent with taurine.

Atrial Gland Peptides.—The atrial gland is an exocrine organ in *A. californica* in which the bioactive peptides are the most widely studied components.³⁶ These peptides have been implicated in the animal's reproductive behavior and may have pheromonal activity.³⁶ Previous studies have shown that the dense-core vesicles of the atrial gland contain high concentrations of bioactive peptides, which result from two precursor proteins designated as the A and B precursors.³⁷ Following processing of the precursors, the resulting atrial gland peptides are N-terminal peptides (A-NTP and B-NTP), peptides A and B, and califins (Figure 1B).^{36,37}

Lysed (underivatized) vesicle extracts were fractionated by HPLC, and collected fractions were assayed for peptide content using MALDI-TOF mass spectrometry. Mass spectra are shown in Figure 6 for collected fractions containing NTPs (Figure 6A), peptides A and B (Figure 6B), and the califins (Figure 6C). The observed m/z values in Figure 6 correlate with the calculated masses from the literature (A-NTP, 1397; peptide A, 3924; peptide B, 4032; califin A, 6144; califin B, 6072).^{36–38} Each califin is composed of a 36-residue peptide linked by a single disulfide bond to an 18-residue fragment.³⁷ The califins degraded quickly, and the eluent had to be stored on dry ice and analyzed within 4 h in order to detect a signal. Degradation of the califins is most likely responsible for the poorer S/N in Figure 6C compared to Figure 6A and B and the absence of the mass corresponding to califin C in this fraction.

Fractions containing the identified peptides were collected from the HPLC column. The eluent is acidic; thus, NaOH was added to the collected fractions, and the pH was estimated (litmus paper) to be pH ~7–8. The pH-adjusted fractions were derivatized with NDA/ CN^- off column and run with CE-LIF. NTPs was positively identified by injecting our purified fraction (Figure 7A) and comparing this to injections of purified NTPs (obtained from G. T. Nagle and S. D. Painter, University of Texas, Galveston, TX) and synthesized A-NTP. Each of these NTP samples gave one sharp peak when run with CE. An electropherogram of a collected fraction containing peptides A and B is shown in Figure 7B. This sample, as well as purified samples of the single peptides (from Nagle and Painter), gives rise to many peaks in the region of NTP with relatively low intensity (compared to Figure 7A). Figure 7C shows an electropherogram of the derivatized HPLC fraction containing the califins. Two main peaks are evident and might correspond to the dissociation of the intact peptides into their 18- and 36-residue fragments. On the basis of Figure 7, the reaction of NDA with the components in the fractions containing peptides A and B and the califins appears to be less efficient than with the NTPs.

NDA reacts with primary amines, and peptides that contain lysine residues are subject to multiple labeling because of the ϵ -amino group of the lysine side chain. The number of possible derivatized products of a peptide containing n total amino groups is $(2^n - 1)$.^{39,40} Consideration of the lysine content of these peptides, in addition to the N-terminus, reveals two, three, four, and two amino groups for NTP, peptide A, peptide B, and the califins, respectively.³⁶ The additional lysine residues in peptides A and B make possible 7 and 15 different derivatized products, respectively, with potentially different electrophoretic mobilities. The nonselective separation conditions and unwanted multiple labeling of lysine residues led to broad bands for peptides A and B and the califins. Consequently, these components were not identified unambiguously in the electropherograms. Poor derivatization efficiency of the peptides in the short reaction time (5 min) probably contributes to the low signal.

Single-Vesicle Identification.

The single-vesicle runs shown in Figure 4B and C reveal important details about the composition of atrial gland vesicles. The observation that taurine is packaged into vesicles as shown in Figure 4B supports the theory that taurine may have neuromodulatory activity.⁴¹ Striking differences are found between parts B and C of Figure 4, in which the presence of peak 4 is accompanied by the absence of taurine, and vice versa. It has been shown by van Heumen et al. that the atrial gland contains three major types of secretory cells.⁴² According to their observations, cell types 1 and 2 both contained secretory granules averaging 1–2- μm diameter, whereas type 3 contained smaller granules of $\sim 0.5 \mu\text{m}$. In our atrial gland dissection and vesicle isolation procedure, we did not distinguish between granules determined to be morphologically different by electron microscopy.⁴² Therefore, it is not surprising that our individual vesicle runs exhibit distinct chemical differences. These differences might be attributed to vesicles from different types of cells or possibly to the same type of vesicle but at a different stage of maturity.⁴²

CONCLUSIONS

We have characterized and identified amine-containing components in single vesicles from the atrial gland of *A. californica* using a combination of optical trapping, CE, and on-column derivatization. The amino acids taurine, alanine, and leucine/isoleucine were positively identified in populations of lysed vesicles. These amino acids were also seen in single-vesicle analyses with CE-LIF. The presence of taurine was confirmed unambiguously in lysed vesicles using HPLC, NMR, CE (with LIF and absorbance), and ESI-MS. Furthermore, observing taurine in single vesicles reveals that this compound is packaged and stored and, therefore, available for secretion upon application of the appropriate stimulus. In addition to amino acids, we also observed the presence of bioactive peptides well-known to be contained in these vesicles. A-NTP, peptides A and B, and califins A and B were identified in lysed vesicle samples using HPLC fractionation and MALDI-TOF mass spectrometry. These peptides were also observed in single-vesicle runs; however, broad bands prevented positive identification of each peptide component. On the basis of our characterization of lysed vesicles and the greater reaction efficiency of NTP over peptides A and B and the califins, we believe that NTP provides the greatest contribution to the peptide band in the electropherograms.

Acknowledgements

We are grateful to Greg T. Nagle and Sherry D. Painter for donating purified atrial gland peptides. We thank Paul Schmier, Rebecca Jockusch, and John Klassen for assistance with ESI-mass spectrometry. S.J.L. acknowledges support from the NIH for a postdoctoral fellowship (GM18386). O.O. is supported by the Swedish Natural Science Research Council (NFR, 10481-305, -308, and -309) and by the Swedish Foundation for Strategic Research (SSF). M.S. is supported by NFR (01-905-313). This work is supported by the International Joint Research Program (NEDO) of

Japan, the U.S. National Institute on Drug Abuse (DA 09873), the National Science Foundation (CHE-9726183), and the National Institutes of Health (1R29GM50336-01A2).

References

1. Hydén, H. In *Biochemistry of the Developing Nervous System, Proceedings of the First International Neurochemical Symposium*; Waelsch, H., Ed.; Academic Press: New York, 1955; pp 358–371.
2. Lowry OH, Roberts NR, Chang MLW. *J Biol Chem* 1956;222:97–107. [PubMed: 13366983]
3. Giacobini E, Zajicek J. *Nature* 1956;177:185–186. [PubMed: 13297009]
4. Giacobini E. *Acta Physiol Scand* 1959;45:238–254. [PubMed: 13827805]
5. Lillard, S. J.; Yeung, E. S. In *The Handbook of Capillary Electrophoresis*, 2nd ed.; Landers, J., Ed.; CRC Press: New York, 1996; pp 523–544.
6. Swanek, F. D.; Ferris, S. S.; Ewing, A. G. In *The Handbook of Capillary Electrophoresis*, 2nd ed.; Landers, J., Ed.; CRC Press: New York, 1996; pp 495–522.
7. Fuller RR, Moroz LL, Gillette R, Sweedler JV. *Neuron* 1998;20:173–181. [PubMed: 9491979]
8. Luzzi V, Lee CL, Allbritton NL. *Anal Chem* 1997;69:4761–4767. [PubMed: 9406526]
9. Nussberger S, Foret F, Hebert SC, Karger BL, Hediger MA. *Biophys J* 1996;70:998–1005. [PubMed: 8789117]
10. Lillard SJ, Yeung ES, McCloskey MA. *Anal Chem* 1996;68:2897–2904. [PubMed: 8794924]
11. Tong W, Yeung ES. *J Chromatogr, B* 1997;689:321–325.
12. Tong W, Yeung ES. *J Neurosci Met* 1997;76:193–201.
13. Bergquist J, Josefsson E, Tarkowski A, Ekman R, Ewing A. *Electrophoresis* 1997;10:1760–1766. [PubMed: 9372267]
14. Bergquist J, Tarkowski A, Ekman R, Ewing A. *Proc Natl Acad Sci USA* 1994;91:12912–12916. [PubMed: 7809145]
15. Hofstadler SA, Severs JC, Smith RD, Swanek FD, Ewing AG. *Rapid Commun Mass Spectrom* 1996;10:919–922. [PubMed: 8777325]
16. Cruz L, Moroz LL, Gillette R, Sweedler JV. *J Neurochem* 1997;69:110–115. [PubMed: 9202300]
17. Garden RW, Shippy SH, Li L, Moroz TP, Sweedler JV. *Proc Natl Acad Sci USA* 1998;95:3972–3977. [PubMed: 9520477]
18. Cahill PS, Walker QD, Finnegan JM, Mickelson GE, Travis ER, Wightman RM. *Anal Chem* 1996;68:3180–3186. [PubMed: 8797378]
19. Pihel K, Hsieh S, Jorgenson JW, Wightman RM. *Anal Chem* 1995;67:4514–4521. [PubMed: 8633786]
20. Schroeder TJ, Borges R, Finnegan JM, Pihel K, Amatore C, Wightman RM. *Biophys J* 1996;70:1061–1068. [PubMed: 8789125]
21. Albillos A, Dernick G, Horstmann H, Almers W, Alvarez de Toledo G, Lindau M. *Nature* 1997;389:509–512. [PubMed: 9333242]
22. Maiti S, Shear JB, Williams RM, Zipfel WR, Webb WW. *Science* 1997;275:530–532. [PubMed: 8999797]
23. Lillard SJ, Yeung ES. *J Neurosci Met* 1997;75:103–109.
24. Chiu DT, Lillard SJ, Scheller RH, Zare RN, Rodríguez-Cruz SE, Williams ER, Orwar O, Sandberg M, Lundqvist JA. *Science* 1998;279:1190–1193. [PubMed: 9469805]
25. Chiu DT, Hsiao A, Gaggar A, Garza-López RA, Orwar O, Zare RN. *Anal Chem* 1997;69:1801–1807. [PubMed: 9164157]
26. Williams ER. *Trends Anal Chem* 1994;13:247–251.
27. Gross DS, Williams ER. *J Am Chem Soc* 1995;117:883–390.
28. Nagle GT, van Heumen WRA, El-Hamzawy MA, Kurosky A. *Peptides* 1994;15:101–108. [PubMed: 8015966]
29. de Montigny P, Stobaugh JF, Givens RS, Carlson RG, Srinivasachar K, Sternson LA, Higuchi T. *Anal Chem* 1987;59:1096–1101.

30. Matuszewski BK, Givens RS, Srinivasachar K, Carlson RG, Higuchi T. *Anal Chem* 1987;59:1102–1105. [PubMed: 3592222]
31. Gilman SD, Ewing AG. *Anal Chem* 1995;67:58–64. [PubMed: 7864392]
32. Zhou SY, Zuo H, Stobaugh JF, Lunte CE, Lunte SM. *Anal Chem* 1995;67:594–599. [PubMed: 7893003]
33. Roach MC, Harmony MD. *Anal Chem* 1987;59:411–415. [PubMed: 3565761]
34. Kwakman PJM, Koelewijn H, Kool I, Brinkman UATh, De Jong GJ. *J Chromatogr* 1990;511:155–166. [PubMed: 2120277]
35. Sossin WS, Kreiner T, Barinaga M, Schilling J, Scheller RH. *J Biol Chem* 1989;264:16933–16940. [PubMed: 2777814]
36. Nagle GT, Painter SD, Blankenship JE, Kurosky A. *J Biol Chem* 1988;263:9223–9237. [PubMed: 3379066]
37. Rothman BS, Hawke DH, Brown RO, Lee TD, Dehghan AA, Shively JE, Mayeri E. *J Biol Chem* 1986;261:1616–1623. [PubMed: 3753705]
38. Lee TD, Legesse K, Hawke DH, Shively JE. *Biochem Biophys Res Commun* 1985;132:520–525. [PubMed: 4062939]
39. Pinto DM, Arriaga EA, Craig D, Angelova J, Sharma N, Ahmadzadeh H, Dovichi NJ. *Anal Chem* 1997;69:3015–3021.
40. Zhao JY, Waldron KC, Miller J, Zhang JZ, Harke H, Dovichi NJ. *J Chromatogr* 1992;608:239–242. [PubMed: 1430027]
41. McCaman R, Stetzler J. *J Neurochem* 1977;29:739–741. [PubMed: 201729]
42. van Heumen WRA, Nagle GT, Kurosky A. *Cell Tissue Res* 1995;279:13–24. [PubMed: 7895254]

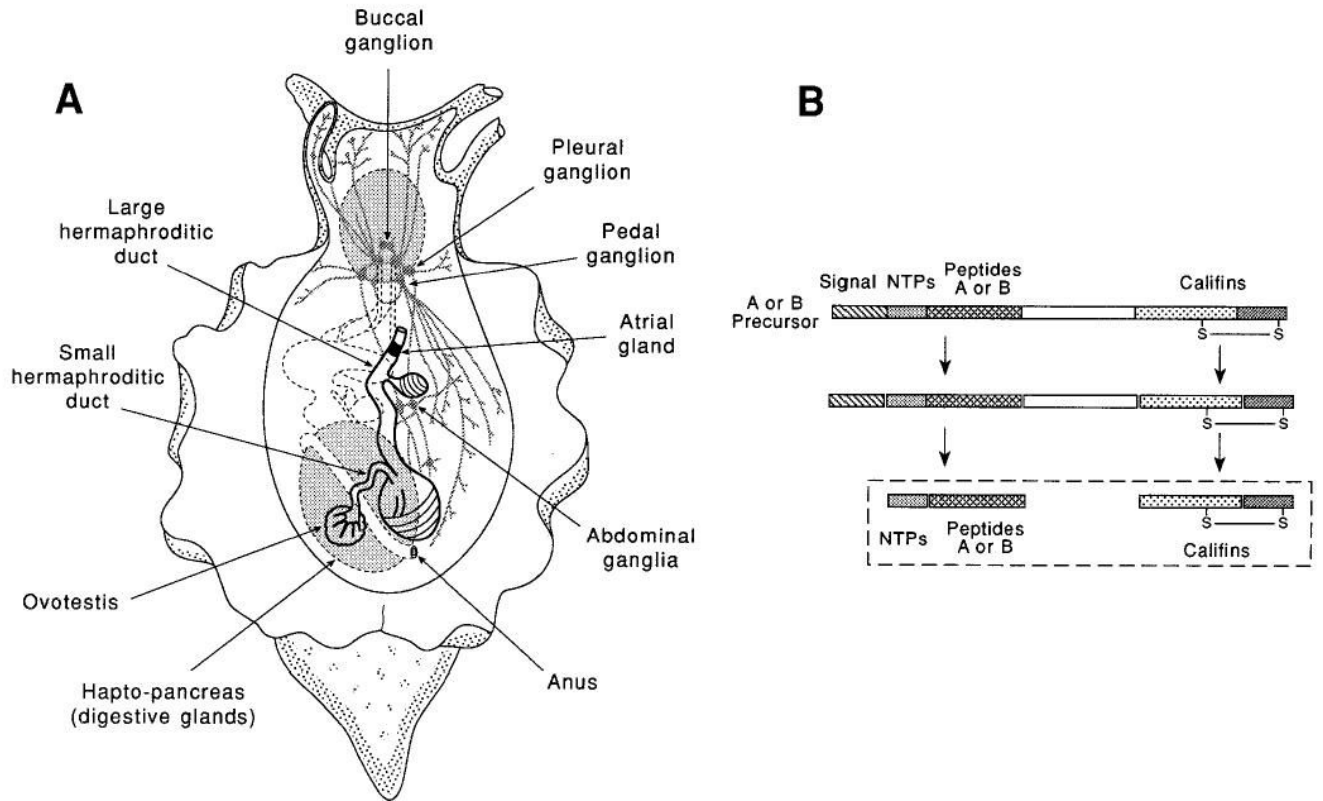


Figure 1. (A) Diagram of *Aplysia californica* showing the location of the atrial gland. (B) Schematic of the precursor and resulting peptides.

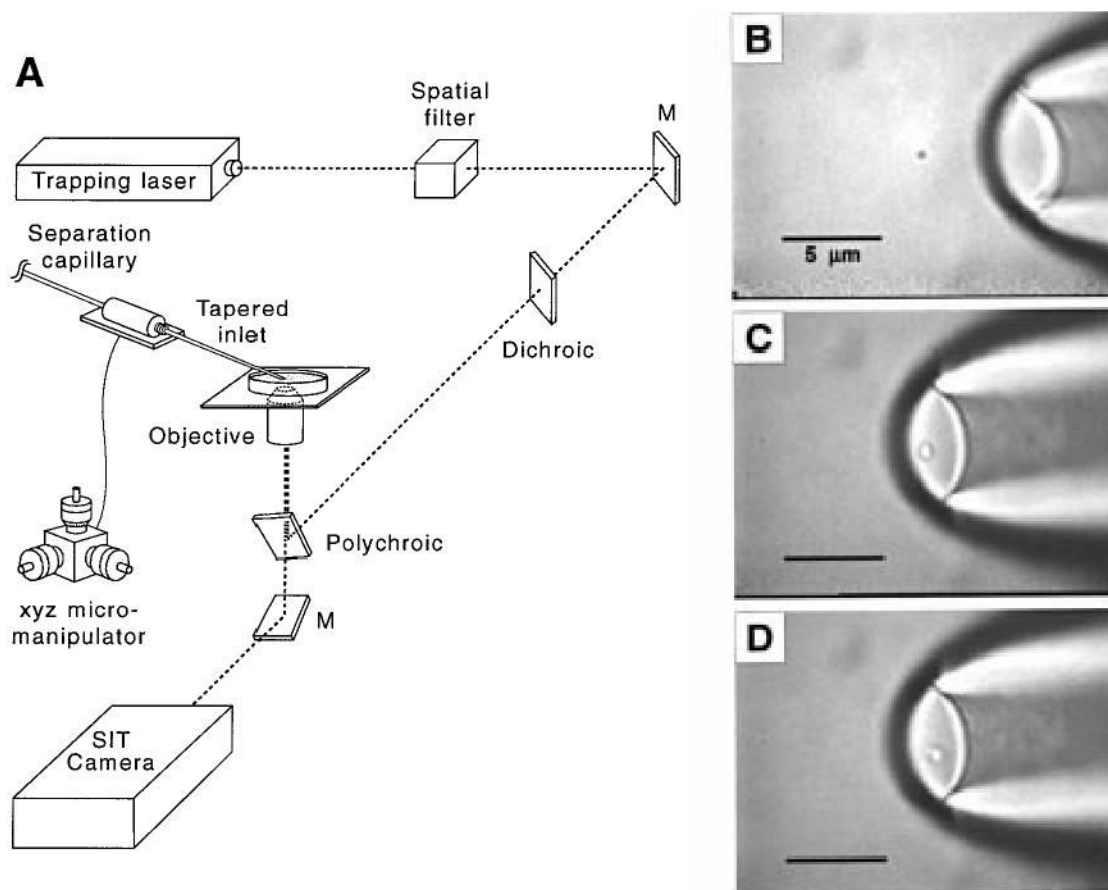


Figure 2. (A) Schematic of optical trap instrumentation. (Note: dichroic and polychroic mirrors were incorporated into this setup because the instrumentation is sometimes used for simultaneous fluorescence microscopy.²⁵) (B) Video image of trapped single vesicle. (C) Image of a single vesicle at the tapered capillary inlet. (D) Image of single vesicle entering the capillary inlet.

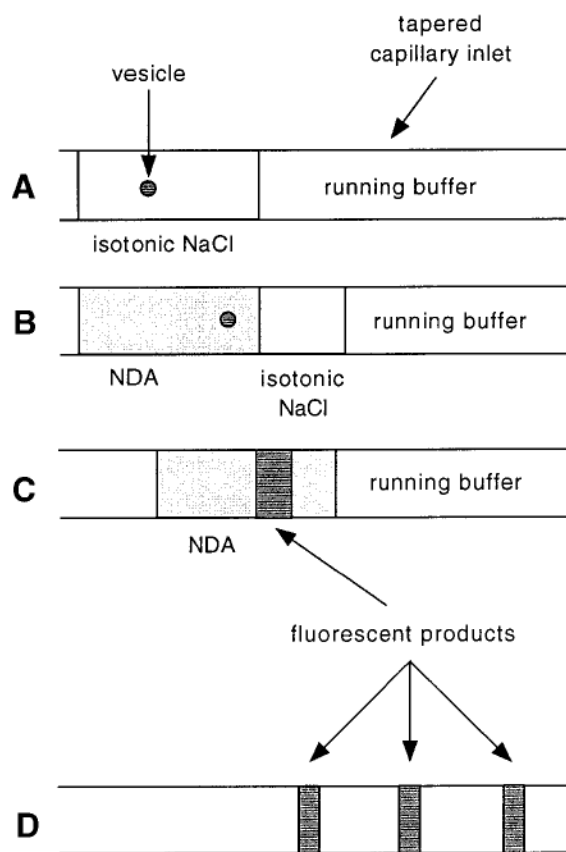


Figure 3. Schematic of on-column derivatization of a single vesicle with NDA/CN⁻. (A) Injection of a plug of isotonic NaCl, followed by a single vesicle, into the tapered inlet. (B) Injection of NDA/CN⁻ into the capillary. (C) Five-minute reaction time to permit lysis of the vesicle and derivatization of its contents. (D) Electrophoresis initiated and the labeled amines separated and detected with CE-LIF.

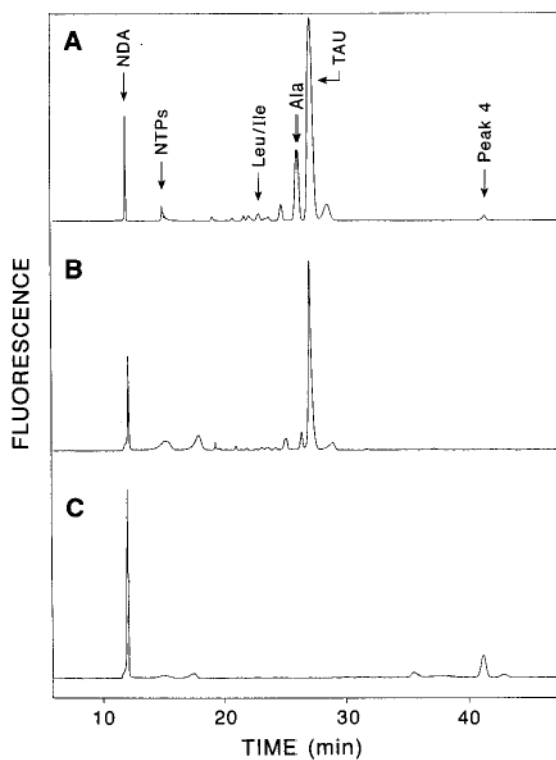


Figure 4. Electropherograms of NDA-derivatized vesicle contents. (A) Lysed sample of population of vesicles in which off-column derivatization was performed. (B) Single vesicle in which taurine is the main component. (C) Single vesicle in which taurine is absent and peak 4 is evident.

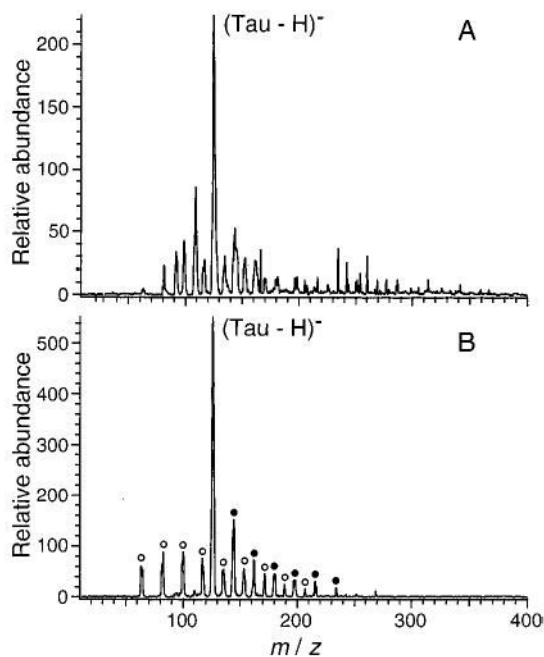


Figure 5. Negative-ion ESI mass spectra. (A) Underderivatized vesicle lysate fractionated with size-exclusion chromatography. (B) Taurine standard solution (1.5×10^{-4} M). Both samples are in 100% H₂O. Filled circles correspond to hydrated (M - H)⁻ taurine ions. Open circles correspond to an impurity (m/z 62) and its hydrated ions present in the taurine sample.

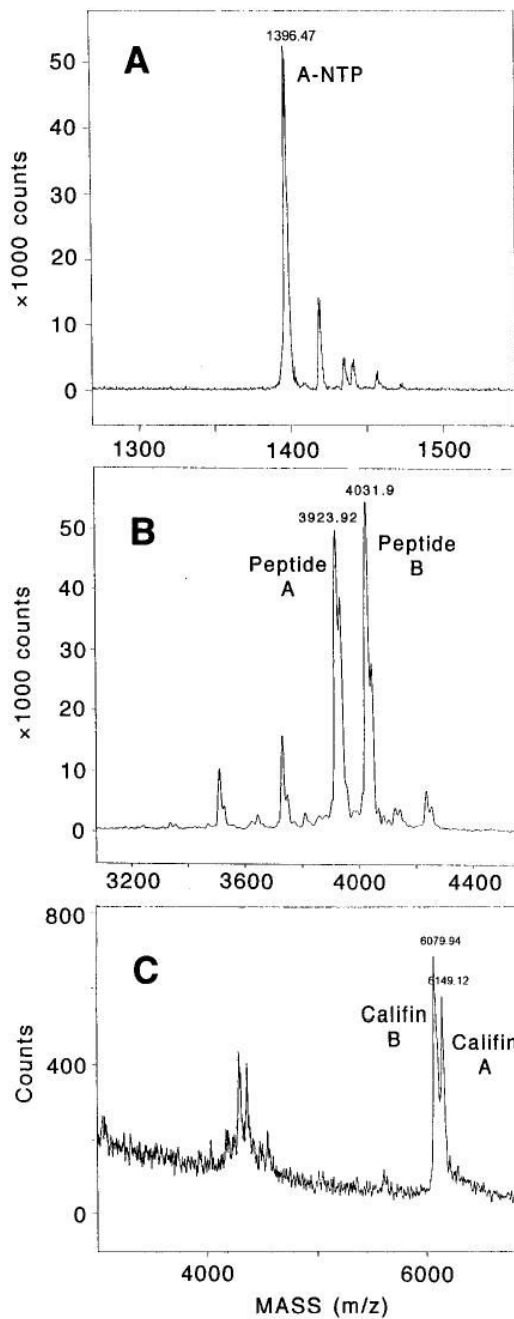


Figure 6. MALDI-TOF mass spectra of fractions collected from HPLC analysis of vesicle lysate showing presence of bioactive peptides. (A) A-NTP, (B) peptides A and B, and (C) califins A and B. Matrixes were α -cyano-4-hydroxycinnamic acid for (A) and sinapinic acid for (B) and (C). Fractions B and C were collected from the same HPLC run; fraction A was collected from a separate HPLC run.

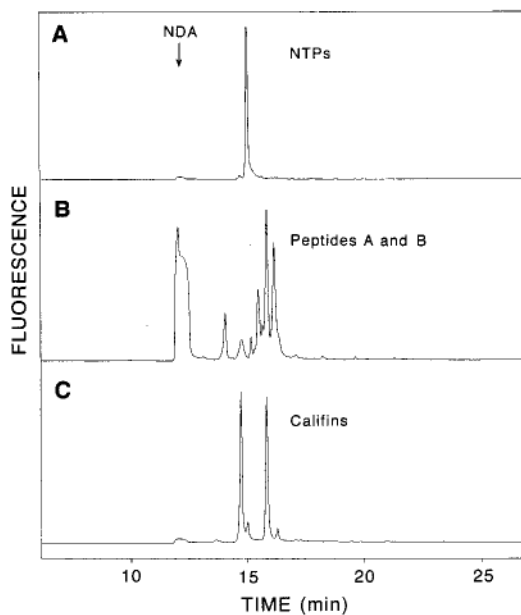


Figure 7. Electropherograms of HPLC fractions containing identified bioactive peptides. Fractions contain (A) NTPs, (B) peptides A and B, and (C) califins. Collected fractions are from an HPLC run different from Figure 6.